Temperature structure functions in the Bolgiano regime of thermal convection

L. Skrbek,[1,2] J. J. Niemela,[1] K. R. Sreenivasan,[3] and R. J. Donnelly[1]

[1]*Cryogenic Helium Turbulence Laboratory, University of Oregon, Eugene, Oregon 97403*
[2]*Low Temperature Laboratory, Institute of Physics ASCR and Charles University, V Holešovičkách 2, 180 00 Prague, Czech Republic*
[3]*Institute for Physical Science and Technology, University of Maryland, College Park, Maryland 20742*

We measure temperature fluctuations in the Rayleigh-Bénard apparatus, which is a closed cylindrical container with the bottom wall heated and the top wall cooled. The aspect ratio, which is the diameter-to-height ratio of the apparatus, is unity. The Rayleigh number is 1.5×10^{11}. The working fluid is cryogenic helium gas. We compute temperature structure functions up to order 16, and use extended self-similarity to obtain scaling exponents in the Bolgiano regime. In contrast to passive scalars, the scaling exponents tend not to saturate with the order of the structure function, suggesting the absence of ramplike structures in temperature traces of convective motion.

I. INTRODUCTION

There is an extensive literature on the scaling properties of structure functions of velocity and temperature fluctuations in turbulent flows. Structure functions are moments of increments of a velocity component, temperature, or some other field variable, across a specified spatial distance r. Kolmogorov's [1] similarity theory predicts that the nth order structure function (i.e., the nth moment of the increment) obeys the scaling law of the form

$$S_n(r) \propto r^{n/3}, \tag{1.1}$$

as long as the separation distance r lies within the inertial range (i.e., between a characteristic dissipation scale and the large scale of turbulence). However, experimental and numerical data show that the scaling exponents depend nonlinearly on n, and fall increasingly short of $n/3$ as n increases [2–4]. This is called anomalous scaling. It is now known that scaling exponents for temperature are more strongly anomalous (e.g., Refs. [4,5]) than those for velocity; when the temperature can be considered a passive scalar, it also appears that the exponents saturate beyond moments of the order 10 [6]. The saturation of the exponents for passive scalars is perhaps linked to the existence of strong ramplike (or shocklike) structures in their time traces. This link is especially clear for a passive scalar advected by a rapidly oscillating velocity field [7–9], and for forced Burgers' equation [10].

The behavior of temperature fluctuations in thermally driven flows such as convection is more complex. Here the state of turbulent motion is determined by the Rayleigh number, Ra, which is a nondimensional measure of the temperature difference between the bottom and top plates of the apparatus, and the Prandtl number, Pr, of the fluid. The Rayleigh number is defined as $\text{Ra} = g\alpha\Delta H^3/\nu\kappa$, where g is the acceleration due to gravity, α is the isobaric thermal expansion coefficient, Δ is the temperature difference between the bottom and top walls separated by a vertical height H, ν is the kinematic viscosity, and κ is the thermal diffusivity of the fluid in the convection apparatus; $\text{Pr} = \nu/\kappa$. In developed thermal convection, corresponding to large values of Ra, two

scaling regions can be observed simultaneously (e.g., Ref. [11]). One of them is the inertial range, in which the effects of buoyancy are not felt directly; the other is the so-called Bolgiano range, in which buoyancy controls the dynamics [12]. The latter range contains scales between the Bolgiano length scale L_B, and the large scale of the system L (which can be regarded as being of the order H). It has been shown in Ref. [13] that L_B can be estimated by

$$L_B = \frac{\varepsilon^{5/4}}{N^{3/4}(g\alpha)^{3/2}} \sim \frac{\text{Nu}^{1/2}H}{(\text{Ra Pr})^{1/4}}, \tag{1.2}$$

where ε is the energy dissipation rate and N is the dissipation rate of temperature variance; Nu denotes the Nusselt number, which is the ratio of the turbulent heat transport to molecular heat transport. The first expression in Eq. (1.2) yields local values of L_B if local dissipation rates are used in the definition, and hence reflects position-dependent values, but the second expression, obtained on dimensional grounds, is an integral quantity characteristic of the entire volume of the apparatus. It should thus be regarded as a characteristic value of L_B.

The scaling properties in the Bolgiano range have been studied only rarely [14]. This work presents an experimental study of this issue. We describe the experimental conditions briefly in Sec. II and discuss the principal results in Sec. III. Some concluding remarks are presented in Sec. IV.

II. THE APPARATUS AND THE MEASUREMENT OF TEMPERATURE FLUCTUATIONS

The Rayleigh-Bénard apparatus is a closed cylindrical container with thick bottom and top walls made of highly conducting [15] annealed copper and thin stainless-steel sidewall. The container is 50 cm in height and 50 cm in diameter (aspect ratio unity). It is essentially the same as that of Ref. [11], except that the height is now halved. By varying the operating temperature and pressure of the working fluid—cryogenic helium gas—together with the temperature difference across the height of the container, Rayleigh num-

bers between 10^6 and 10^{16} can be generated in the present setup. We placed several sensors in various positions inside the container [11], but the present analysis uses data from a sensor [16] placed very close to the center plane of the apparatus, at a distance of 4.4 cm from the side wall. The sensor was operated on a bridge circuit, whose resistance fluctuations, sampled at 50 Hz, were converted into temperature fluctuations by means of an appropriate calibration curve. We used a dual-phase lock-in amplifier operating at frequencies of few kHz and time constant of approximately 30 ms. It is generally understood that the signal is true only on time scales larger than a multiple of this time constant; we pay particular attention to this constraint in the following analysis. Each data file contains 2^{19} samples, and 44 such records, consecutively measured under steady external conditions, were analyzed.

While we compute structure functions with time increments, we interpret them towards the end of the paper as having been obtained with space increments by invoking Taylor's frozen flow hypothesis. This interpretation is needed for making contact with existing literature and tradition. The persistence of a strong mean wind at the point of measurement makes this interpretation plausible. (The mean wind weakens as one approaches the core of the apparatus.) The situation is somewhat complicated by the fact that the wind switches direction abruptly and irregularly [17] towards high Rayleigh numbers. Operationally, frozen flow hypothesis requires that the direction of the wind be stable for periods of time large compared to the turnover time of the mean wind— this being a characteristic of the large scale. For Ra=1.5 $\times 10^{11}$, the average time interval between reversals is about 300 s, while the turnover time of the biggest roll is about 30 s (wind velocity is about 7 cm/s, and the perimeter of the apparatus is 200 cm). Our criterion is thus satisfied. At much higher Ra, the tendency of the wind to reverse its direction more frequently [17] invalidates the criterion. Thus, the Rayleigh number is held fixed at 1.5×10^{11} for the present analysis, although measurements have been made for Rayleigh numbers that are several orders of magnitude larger [11].

III. EXPERIMENTAL RESULTS

For purposes of this study we converted temperature fluctuations into a standard form with zero mean and unity standard deviation. For useful reference, we present in Fig. 1 the histogram of the temperature. Its overall shape is skewed with broad "shoulders," perhaps resembling Gaussianity for fluctuations smaller than one standard deviation from the mean (see inset). The shape for rare events is roughly exponential. The histogram is different from that measured at the geometrical center of the apparatus, where it is nearly Gaussian for low Ra and evolves towards a stretched exponential shape for higher Ra [18,11]. Its peculiar shape in Fig. 1 is thus a consequence of the mean wind.

We have calculated structure functions of orders n =1–4, 6, 8, 10, 12, and 16, for discrete time intervals $m\Delta t$, using the definition

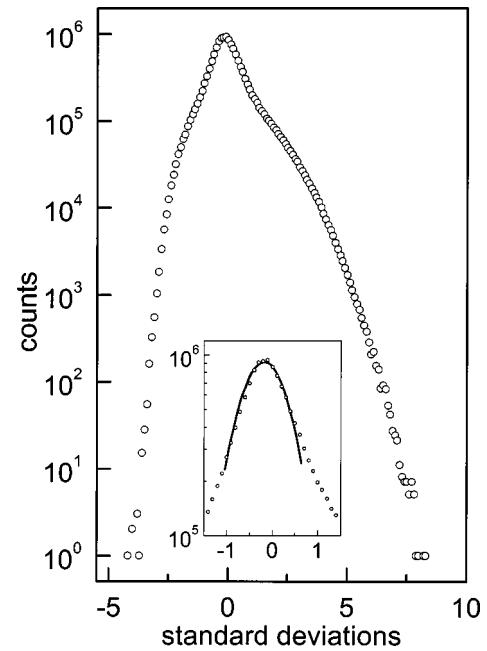$$S_n^t(m\Delta t) = \langle |\theta(t_0 + m\Delta t) - \theta(t_0)|^n \rangle, \qquad (3.1)$$

FIG. 1. The histogram of the temperature plotted in units of its standard deviation for 14 data files (each containing 2^{19} samples). Two hundred bins, each of which is $\frac{1}{10}$th of the standard deviation, have been used. The inset expands the histogram around the mean, plotted in logarithmic units and compared to a parabola to judge the degree of Gaussianity.

where $\Delta t = 1/50$ s, corresponding to the sampling frequency of 50 Hz. We have computed structure functions for absolute values of temperature differences to avoid possible cancellation effects that might occur due to wind reversal.

We plotted structure functions for each set of data and inspected them. Typical variability of structure functions computed from 14 illustrative records are shown in Fig. 2. Low-order structure functions, up to order four, are similar to each other. The differences between records increase for high-order structure functions; in fact, a few data sets showed unreasonably large departures from the overall trend of Fig. 2. We do not understand the reason for such strong deviations, but suspect that they come from occasional electronic spikes. It is well known that even a few such points will affect high-order structure functions. We have therefore excluded such records. This may prejudice the results by excluding genuinely rare physical events, but we think that this is unlikely because each record is about 350 turnover times in duration, and we have processed as many as 32 independent files.

Let us first examine the behavior of the structure functions for large time increments. All of them, particularly the low-order ones, display oscillations, as shown expanded in Fig. 3. It is natural to associate the three minima in Fig. 3 with one, two, and three full rotations of the mean wind. The time shift of the first minimum corresponds to $\tau_{\text{rot}} \approx 27.4$ s, the second and the third minima being its multiples. Since the mean wind is in the form of a horizontal roll of the size of the apparatus, we can estimate the mean velocity roughly as 200 cm/27.4 s ≈ 7.3 cm/s, in good agreement with our previous independent measurement [17]. We therefore conclude
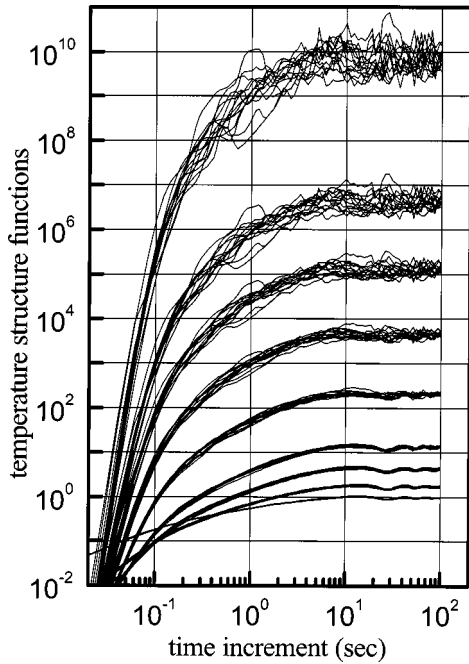
FIG. 2. Temperature structure functions of order 1–4, 6, 8, 10, 12, and 16 (the order increasing upwards) calculated for 14 data files, plotted against time in seconds.

that structure functions for large time increments contain information about the mean wind. Further, the characteristic decay of the amplitudes of these peaks indicates the existence of a much longer time scale in the flow. This feature has been discussed in a different study focusing on the properties of the mean wind [19].
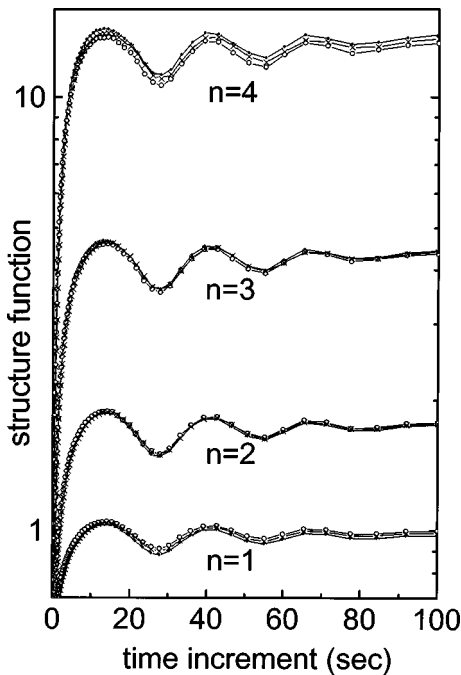

FIG. 3. Temperature structure functions of order 1, 2, 3, and 4. The oscillation minima correspond to one, two, and three turnover times of the mean wind.
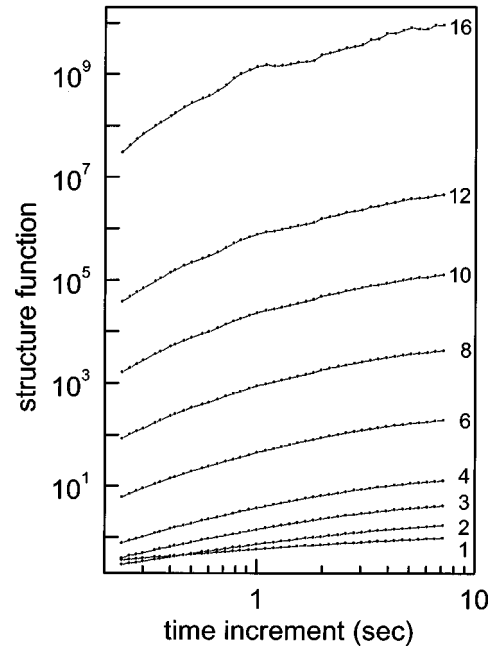

FIG. 4. Temperature structure functions of the indicated order, calculated from 14 data files. The time increment spans the Bolgiano range estimated in the text. Filled circles are from the sensor (26 data files). Other symbols correspond to data from a second sensor placed nearby.

As already mentioned, our principal interest is in the Bolgiano range of scales. According to Eq. (1.2), using the measured $Nu \approx 350$ and $Pr \approx 0.7$, we estimate $L_B \approx 1.5$ cm or, converting space to time through the mean wind, that τ_B is about 0.2 s. A scale of the order of the height of the apparatus is equivalent to τ_{out} of about 7 s. It is in the range between τ_B and τ_{out} that we hope to find Bolgiano scaling. Therefore, for further analysis we plot data for 0.2 s$<\tau<10$ s. The averaged structure functions are shown in Fig. 4 for this range of τ.

Figure 4 shows that the scaling is ambiguous at best, especially for high orders. We therefore consider extended self-similarity (ESS) [20]. Let us first follow the approach of Ching [21] and plot the ratio $S_1/\sqrt{(S_2)}$ versus time increment. Figure 5 shows that scaling indeed exists in the entire Bolgiano range (indicated between arrows at τ_B and τ_{out}), with an exponent of 0.057. Note that this type of plot also displays oscillations for larger scales.

Figure 6 shows structure functions up to order $n=8$ plotted in the ESS manner, namely S_n versus S_2, averaged over 26 data files. The data lying within the Bolgiano range are highlighted. Reasonable scaling can be found although it deteriorates with increasing moment order. The oscillations due to the mean wind have essentially disappeared (but can be inferred from the clustering of points towards large values of S_2). Indeed, scaling can be found whenever the nth order structure function is plotted against the mth order, n and m being arbitrary within the range considered here. The best linear fits for all possible combinations of S_n versus S_m were obtained. The resulting ESS exponents ζ_n^m are presented in Table I.
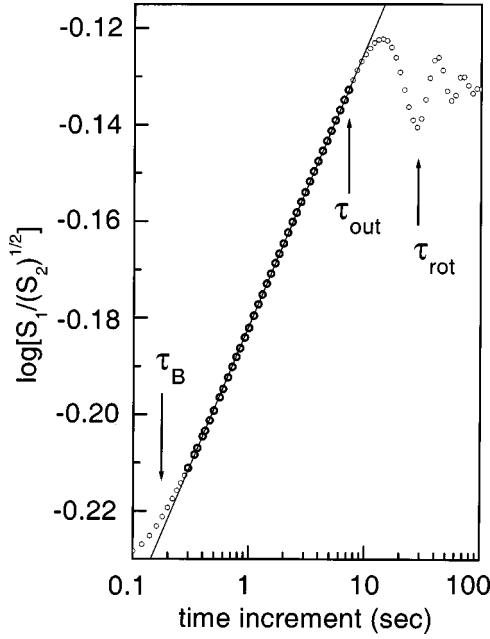
FIG. 5. The logarithm to base 10 of the ratio $S_1/\sqrt{(S_2)}$, calculated using 26 data files, plotted versus time increment; those within the expected Bolgiano range are highlighted. The characteristic times τ_B, τ_{out}, and τ_{rot} are defined in the text.

Using the exponents from Table I we can check the consistency of the data. For example, the scaling exponent ζ_1^{16} $=S_{16}/S_1 \approx 4.63$. For self-consistency, one should also be able to obtain this same number by decomposing ζ_1^{16} as $\zeta_{12}^{16}\zeta_{10}^{12}\zeta_8^{10}\zeta_6^8\zeta_4^6\zeta_3^4\zeta_2^3\zeta_1^2 = 4.71$. These two estimates differ by
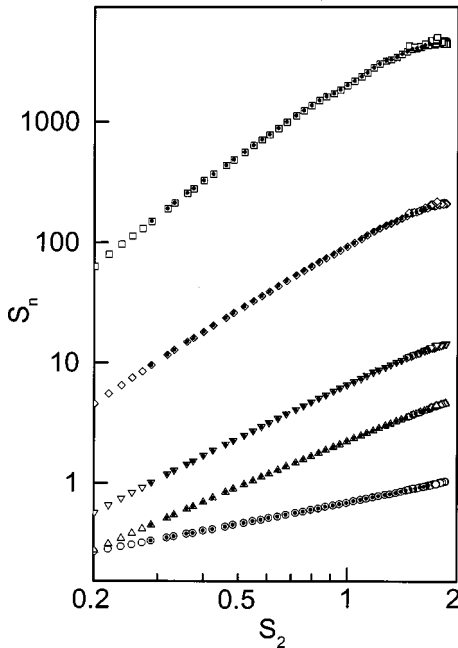

FIG. 6. Temperature structure functions of order 1, 3, 4, 6, and 8 (order increasing upwards) for 26 data files, plotted against the second-order structure function S_2. The data points within the Bolgiano range are highlighted.

1.7%. One can check that this test works in many different ways, for example, $\zeta_1^{16}=\zeta_{12}^{16}\zeta_1^{12}=4.67$, which agrees well with the other two estimates. Indeed, all such self-consistency checks are satisfied to within about 2%. This self-consistency is obviously satisfied if ESS holds accurately. Since log-log plots do not have adequate resolution to verify this feature, it is important to know that these self-consistency checks indeed work. This self-consistency of exponents implies, as well, the validity of the so-called generalized self-similar scaling [22].

The scaling exponents obtained relative to ζ_2 are plotted in Fig. 7. They show strong intermittency of the temperature field but show no tendency to saturate, at least for n up to order 16.

It is interesting to compare the present ESS exponents with those obtained in the inertial range, in essentially isothermal turbulence generated in a wind tunnel, for the velocity and passive temperature fluctuations. As an example, we have chosen the data of Ruiz-Chavarria *et al.* [5] who obtained both velocity and temperature data in the turbulent wake of a circular cylinder. Temperature fluctuations were produced by heating an array of thin wires placed downstream of the cylinder. As is known previously, the velocity data agree well with the She-Leveque prediction [23] (see Fig. 7). For the temperature field, the high-order scaling exponents deviate increasingly from those of the velocity field, in accordance with the notion that the temperature field is more intermittent. Up to order 6, the data of Ref. [5] and
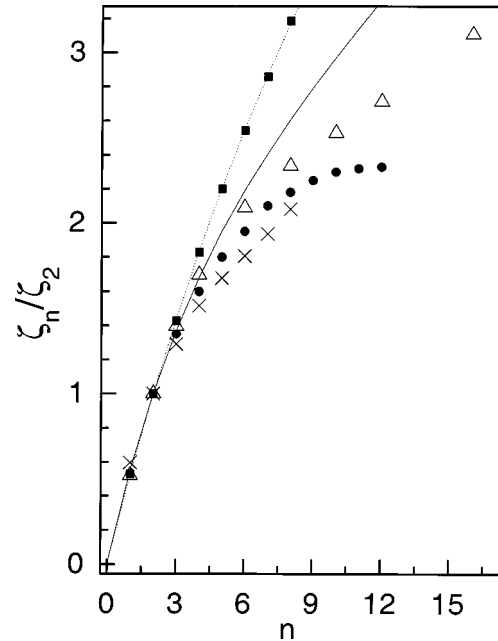

FIG. 7. The ratio of the relative scaling exponents ζ_n/ζ_2 plotted versus the order of the structure function n. Open triangles denote the present data (26 data files). They are compared with structure functions for velocity (■) and temperature (×) from Ref. [5], and for passive temperature data (dark circles) from Ref. [6]. The dotted line is the result from the model of Ref. [23] for velocity, and is given by $\xi_n=n/9+2[1-(2/3)^{n/3}]$; the solid-line is the complementary result of Leveque *et al.* [24] for temperature, given by ζ_n $=n/9+(10/9)[1-(2/5)^{n/3}]$.

TABLE I. Experimental values of exponents, obtained from best linear fits to structure functions of various orders, plotted against each other on log-log coordinates. Data from 26 files have been used. Here, N can be either n or m.

N	1	2	3	4	6	8	10	12	16
1	1								
2	1.921	1							
3	2.678	1.396	1						
4	3.253	1.697	1.217	1					
6	4.002	2.090	1.500	1.233	1				
8	4.470	2.336	1.677	1.379	1.119	1			
10	4.838	2.528	1.815	1.493	1.212	1.083	1		
12	5.186	2.711	1.947	1.602	1.300	1.162	1.073	1	
16	5.934	3.107	2.231	1.836	1.490	1.333	1.232	1.150	1

those of [6] compare well though they deviate for higher orders. They both fall short of the modified prediction of Leveque *et al.* [24] for passive scalars. The present exponents, unlike those of Moisy *et al.* [6] for the passive temperature field between rotating discs, do not show a tendency to saturation.

IV. CONCLUDING REMARKS

In order to study the scaling properties of the temperature field in highly turbulent thermal convection, we have analyzed long records of temperature in thermal convection at a fixed Ra $= 1.5 \times 10^{11}$. This value of Ra was chosen as a compromise between two opposing requirements: the requirement of the highest possible Ra for purposes of obtaining the largest scaling range, and the propensity for the mean wind to oscillate rapidly as the Rayleigh number increases. Generally, it was not possible to observe any scaling without using ESS. All our exponents are thus relative to some reference moment. The exponents obtained with different reference moments are self-consistent to within an accuracy of the order of 2%. In particular, those computed relative to the second-order structure function show no tendency to satura-

tion, in contrast to the trend seen in Ref. [6] for the passive temperature field in the inertial range of a flow between counterrotating discs. This is a basic difference between active and passive scalars. This feature reflects the fact that, for active scalars, ramplike structures are likely absent on scales within the Bolgiano range. Inspection of temperature traces supports this conclusion. Further, the Boussinesq equation can be used to show that ramplike structures in the temperature are unlikely [25]. Simple rewriting of the equation shows that the combination of the fluid acceleration and pressure gradient yields the fluid temperature (modulo the gravitational acceleration). Since pressure prevents ramplike objects from forming, it is reasonable to expect that the active temperature does not exhibit such shapes. It will be useful to check this conclusion from data obtained elsewhere in the convection cell.

[1] A. N. Kolmogorov, Dokl. Akad. Nauk SSSR **30**, 301 (1941).

[2] R. A. Antonia, E. Hopfinger, Y. Gagne, and F. Anselmet, Phys. Rev. A **30**, 2704 (1984).

[3] U. Frisch, *Turbulence* (Cambridge University Press, Cambridge, 1995).

[4] K. R. Sreenivasan and R. A. Antonia, Annu. Rev. Fluid Mech. **29**, 435 (1997).

[5] G. Ruiz-Chavarria, C. Baudet, and S. Ciliberto, Physica D **99**, 369 (1996).

[6] F. Moisy, H. Willaime, J. S. Andersen, and P. Tabeling, Phys. Rev. Lett. **86**, 4827 (2001).

[7] M. Chertkov, Phys. Rev. E **55**, 2722 (1997).

[8] V. Yakhot, Phys. Rev. E **55**, 329 (1997).

[9] E. Balkovsky and V. Lebedev, Phys. Rev. E **58**, 5776 (1998).

[10] V. Yakhot and A. Chekhlov, Phys. Rev. Lett. **77**, 3118 (1996).

[11] J. J. Niemela, L. Skrbek, K. R. Sreenivasan, and R. J. Donnelly, Nature (London) **404**, 837 (2000).

[12] A. S. Monin and A. M. Yaglom, *Statistical Fluid Mechanics* (MIT Press, Cambridge, MA, 1975), Vol. 2.

[13] F. Chillà, S. Ciliberto, C. Innocenti, and E. Pampaloni, Nuovo Cimento D **15**, 1229 (1993).

[14] K. Aivalis, K. R. Sreenivasan, Y. Tusji, J. Klewecki, and C. Biltoft, Phys. Fluids **14**, 2439 (2002).

[15] The heat conductivity of the bottom and top plates was estimated *in situ* to be not less than 2 kW m^{-1} K^{-1} at an operating temperature of 5 K.

[16] The sensors are made of neutron-doped germanium crystals and 250 μm on the side. Their resistance is $R \approx 2$ kΩ and the temperature sensitivity is typically $dR/dT \approx 1$ Ω/mK around 5 K.

[17] J. J. Niemela, L. Skrbek, K. R. Sreenivasan, and R. J. Donnelly, J. Fluid Mech. **449**, 169 (2001).

[18] B. Castaing, G. Gunaratne, F. Heslot, L. Kadanoff, A. Libchaber, S. Thomae, S. X. Wu, S. Zaleski, and G. Zanetti, J. Fluid

Mech. **204**, 1 (1989).

[19] K. R. Sreenivasan, A. Bershadskii, and J. J. Niemela, Phys. Rev. E **65**, 056306 (2002).

[20] R. Benzi, S. Ciliberto, R. Tripiccione, C. Baudet, F. Massaioli, and S. Succi, Phys. Rev. E **48**, R29 (1993).

[21] E. S. C. Ching, Phys. Rev. E **61**, R33 (2000).

[22] R. Benzi, L. Biferale, S. Ciliberto, M. V. Struglia, and R. Tripiccione, Physica D **96**, 162 (1996).

[23] Z.-S. She and E. Leveque, Phys. Rev. Lett. **72**, 336 (1994).

[24] E. Leveque, G. Ruiz-Chavarria, C. Baudet, and S. Ciliberto, Phys. Fluids **11**, 1869 (1999).

[25] V. Yakhot (private communication).